

Toward Clean and Crackless Transfer of Graphene

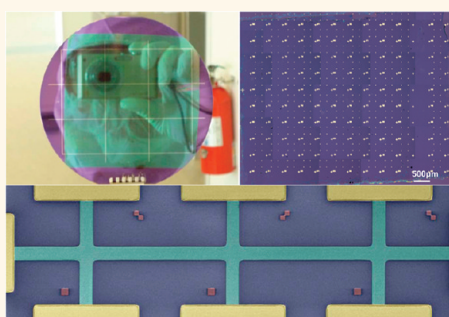
Xuelei Liang,^{†,‡,*} Brent A. Sperl,[†] Irene Calizo,[†] Guangjun Cheng,[†] Christina Ann Hacker,[†] Qin Zhang,[†] Yaw Obeng,[†] Kai Yan,[§] Hailin Peng,[§] Qiliang Li,[⊥] Xiaoxiao Zhu,[⊥] Hui Yuan,[⊥] Angela R. Hight Walker,[†] Zhongfan Liu,[§] Lian-mao Peng,[‡] and Curt A. Richter^{†,*}

[†]National Institute of Standards and Technology, Gaithersburg, Maryland 20899, United States, [‡]Key Laboratory for the Physics and Chemistry of Nanodevices and Department of Electronics, Peking University, Beijing, 100871, China, [§]College of Chemistry and Molecular Engineering, Peking University, Beijing 100871, China, and [⊥]Department of Electrical and Computer Engineering, George Mason University, Fairfax, Virginia 22030, United States

Graphene is regarded as a promising material that could be the basis for future generations of low-power, faster, and smaller electronics.^{1,2} In order for graphene to fulfill this promise and become a material for the large-scale manufacture of high-performance electronics, large-area, high-quality graphene on substrates amenable to electrical device operation and integrated circuit fabrication is needed. For example, with current mass production of Si technology based on 300 mm diameter wafers, methods are sought that can reproducibly afford high-quality graphene films with areas on the order of 0.1 m². Since graphene was first demonstrated by mechanical exfoliation,³ several methods have been developed for producing graphene.^{4–7} Among those methods, only epitaxial growth on the SiC surface (which is limited by the size of high-quality SiC substrates)⁴ and chemical vapor deposition (CVD) on the surface of transition metals^{5,6} can be combined with standard wafer-scale lithographic methods and are compatible with the current integrated circuit fabrication processes.⁷ Large-area graphene as nickel and copper by the CVD method,^{5,6} with continuous graphene films up to 30 in. diagonal having been demonstrated.⁸ Considering its low cost and high efficiency, this CVD method is the most promising approach for producing graphene for large-scale electronic device applications. By optimizing the growth conditions, the quality of such CVD-grown graphene could match that of graphene epitaxially grown on SiC.⁹

The first step necessary in fabricating devices from CVD-grown graphene is to transfer the graphene from the metal growth substrate onto a device-compatible substrate (typically an insulator). It is crucial

ABSTRACT



We present the results of a thorough study of wet chemical methods for transferring chemical vapor deposition grown graphene from the metal growth substrate to a device-compatible substrate. On the basis of these results, we have developed a “modified RCA clean” transfer method that has much better control of both contamination and crack formation and does not degrade the quality of the transferred graphene. Using this transfer method, high device yields, up to 97%, with a narrow device performance metrics distribution were achieved. This demonstration addresses an important step toward large-scale graphene-based electronic device applications.

KEYWORDS: graphene transfer · clean · crackless · high device yields · narrow performance metrics distribution

to device performance, yield, and uniformity that the quality of the graphene is not degraded during this transfer process. Thus, in an ideal transfer process, the graphene film should remain clean (*i.e.*, with no contamination) and continuous (*i.e.*, without folds, cracks, or holes). One common method for transferring graphene from a transition metal growth substrate is the “PMMA-mediated” approach.^{10–12} In this method a layer of poly(methyl-methacrylate) (PMMA) is coated onto the graphene, and the metal below it is etched away completely by etchant. The PMMA/graphene stack is then transferred onto another substrate, and solvents are used to remove the PMMA

* Address correspondence to liangxl@pku.edu.cn; curt.richter@nist.gov.

Received for review September 1, 2011 and accepted October 16, 2011.

Published online October 16, 2011 10.1021/nn203377t

© 2011 American Chemical Society

and complete the graphene transfer. This approach is relatively simple, making it a popular transfer method. Recently a “roll-to-roll” analogue of the PMMA-mediated method was demonstrated⁸ in which thermal release tape was used instead of PMMA. While the thermal-release-tape-assisted method might be easier to scale up to very large areas, it invariably contaminates the transferred graphene surface with adhesive from the thermal release tape.⁸ These residues are difficult to clean and will negatively affect the performance of devices fabricated from graphene transferred in this manner.

Copper is commonly used as a substrate for CVD growth of graphene, while the popular chemical etchants for graphene transfer include aqueous solutions of iron nitrate,⁵ iron chloride,⁶ and ammonium persulfate.⁸ Although these three etchants can effectively remove copper substrate, the resulting graphene films tend to be contaminated with oxidized metal particulates, which could not be washed off in the cleaning system used. When the graphene is transferred onto a device substrate, this metal-based contamination is trapped at the graphene/substrate interface, where it cannot be cleaned with further processing. These trapped contaminants tend to act as scattering centers and degrade carrier transport properties and subsequently device performance. Controlling this contamination is a major challenge associated with the current graphene transfer processes. Another common and important issue during the transfer process is the introduction of cracks and tears into graphene films, which will significantly decrease device yields. Thus, an improved graphene transfer process that better controls contamination and crack formation is a critical advancement necessary for the development and eventual commercialization of high-performance electronics based upon graphene.

In this paper, we present a “modified RCA (Radio Corporation of America) clean” transfer method, which combines an effective metal cleaning process with control of the hydrophilicity of target substrates to better control both contamination and crack formation relative to the traditional approaches. This optimized approach does not appear to degrade the electrical quality of the transferred graphene significantly. High device yields, up to 97%, with narrow device performance metrics distributions were achieved by using this transfer method.

RESULTS AND DISCUSSION

In this work to develop an optimal graphene transfer method, we focus on the “PMMA-mediated” transfer method, as it avoids the organic adhesive residues introduced by thermal release tape in roll-to-roll techniques. After coating PMMA, large-area graphene/Cu

samples were cut into coupons for transfer process development. When Cu is etched away by iron nitrate ($\text{Fe}(\text{NO}_3)_3$), the transparent PMMA/graphene stack usually floats on the solution surface. In the traditional “PMMA-mediated” transfer, the floating PMMA/graphene stack is scooped out directly onto the target substrate. PMMA is then removed by solvent rinsing (such as acetone or *n*-methylpyrrolidinone). We investigated the quality of the graphene after transfer by this traditional method. Although the graphene films transferred by this approach superficially appear clean under moderate magnification optical microscopy (Figure 1a), there are still many micrometer-sized residual particles observable at higher magnifications, as shown in Figure 1b (see Supporting Information Figure S1b). Even when the PMMA-mediated samples appear clean when viewed in an optical microscope, a high density of residual particles is observed when the samples are examined in a scanning electron microscope (SEM), as shown in Figure 1c (see Supporting Information Figure S1c). Furthermore, in some instances a thin layer of residue is observed in samples where the PMMA/graphene stack was not rinsed thoroughly by DI water (see Supporting Information Figure S1d). These residues most probably originated in the Cu etching process and are intolerable for large-scale electronic device or circuit fabrication. Therefore, a transfer process that leads to significantly cleaner transferred graphene films is necessary.

RCA cleans are ubiquitous Si wafer cleaning techniques in semiconductor manufacturing;¹³ thus it seems natural to apply the same techniques to graphene transfer. Traditional RCA cleans usually involve three sequential steps: Step 1, referred to as standard clean 1 (SC-1), is intended for the removal of insoluble organic contaminants with a 5:1:1 $\text{H}_2\text{O}/\text{H}_2\text{O}_2/\text{NH}_4\text{OH}$ solution; step 2 is an oxide strip using a diluted 50:1 $\text{H}_2\text{O}/\text{HF}$ solution to remove a thin silicon dioxide layer where metallic contaminants may have accumulated as a result of step 1; and step 3, standard clean 2 (SC-2), removes ionic and heavy metal atomic contaminants by using a solution of 5:1:1 $\text{H}_2\text{O}/\text{H}_2\text{O}_2/\text{HCl}$. Since step 2 is intended for the removal of a silicon dioxide layer, it is not applicable to the cleaning of the PMMA/graphene stack and was thus eliminated from the cleaning sequence adopted in this work. SC-1 and SC-2 are traditionally performed at process temperatures around 80 °C, which is unsuitable for the graphene transfer process because the bubbles generated from the decomposition of H_2O_2 in these aggressive solutions tear and damage the fragile PMMA/graphene stack. We adapted both the SC-1 and SC-2 solutions for cleaning the graphene films by diluting them to 20:1:1 and operating at room temperature. There was no indication that the PMMA film was attacked by such diluted solutions at room temperature. We also perform

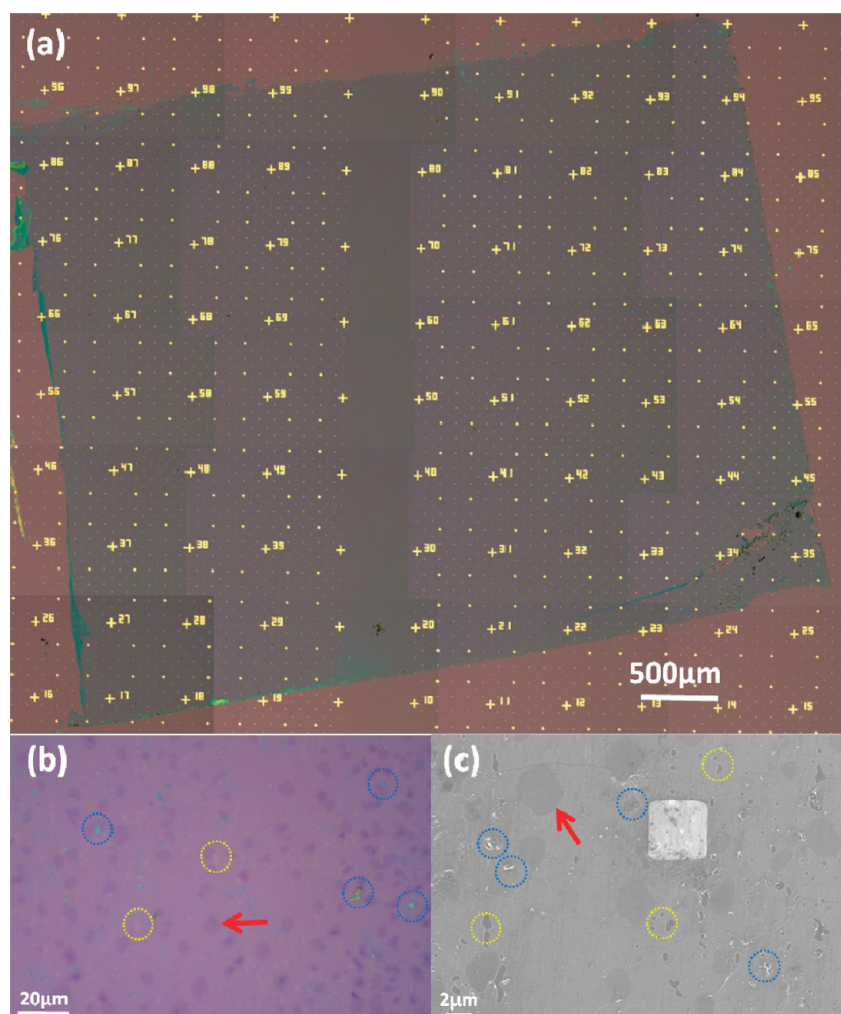


Figure 1. (a) Optical image of a graphene film on a Si/SiO₂ substrate transferred by the traditional “PMMA-mediated” method. The crack at the bottom right corner was introduced by tweezers when handling the sample before the Cu etch. (b) Typical high-magnification optical and (c) SEM images of graphene films shown in (a). Many residual metal particles (for example, blue circles) and small holes (for example, yellow circles) can be seen. Some multilayer graphene areas (with darker contrast) are marked by arrows.

the SC-2 step first because cleaning the residual metal particles remaining on the PMMA/graphene stack is the first priority, and we found reversing the cleaning steps in this manner yielded superior results. After each etching step, the PMMA/graphene stack was rinsed by DI water. Since the adapted RCA clean steps were added to the PMMA-mediated graphene transfer process, we refer to this as the “modified RCA clean” transfer process, and all subsequent references to “RCA clean” in this paper refer to this “modified RCA clean”. Typical images of transferred graphene film are shown in Figure 2 (see Supporting Information Figure S2b). The transferred graphene film is very clean, with almost no residual particles seen under optical microscope. The thin layer of residue was never observed after the RCA clean. In fact, when the PMMA/graphene stack was transferred into the DI water for rinse after the SC-2 step, it already looked much cleaner and more transparent even to the naked eye than before the SC-2 clean.

A scanning electron microscope was used to determine if submicrometer-sized residual particles remain on the graphene that cannot be seen by using optical microscopy; typical results are shown in Figure 2c (see Supporting Information Figure S2c). Some nanoparticles with sizes less than 100 nm were observed. The large metal residual particles (as seen in Figure 1) were rarely observed even after searching the entire graphene area. The nanoparticles appear only on the surface of some as-grown graphene samples and are never observed on the copper foil surface before growth (see Supporting Information Figure S3). We believe these nanoparticles formed during the CVD graphene growth process and were not the Cu substrate etching residues remaining from the transfer process. More detailed work on the origin of these small particles is ongoing and is beyond the scope of this paper. Growth processes must be optimized to avoid producing these nanoparticles. In addition to these nanoparticles, some dark lines were also seen in

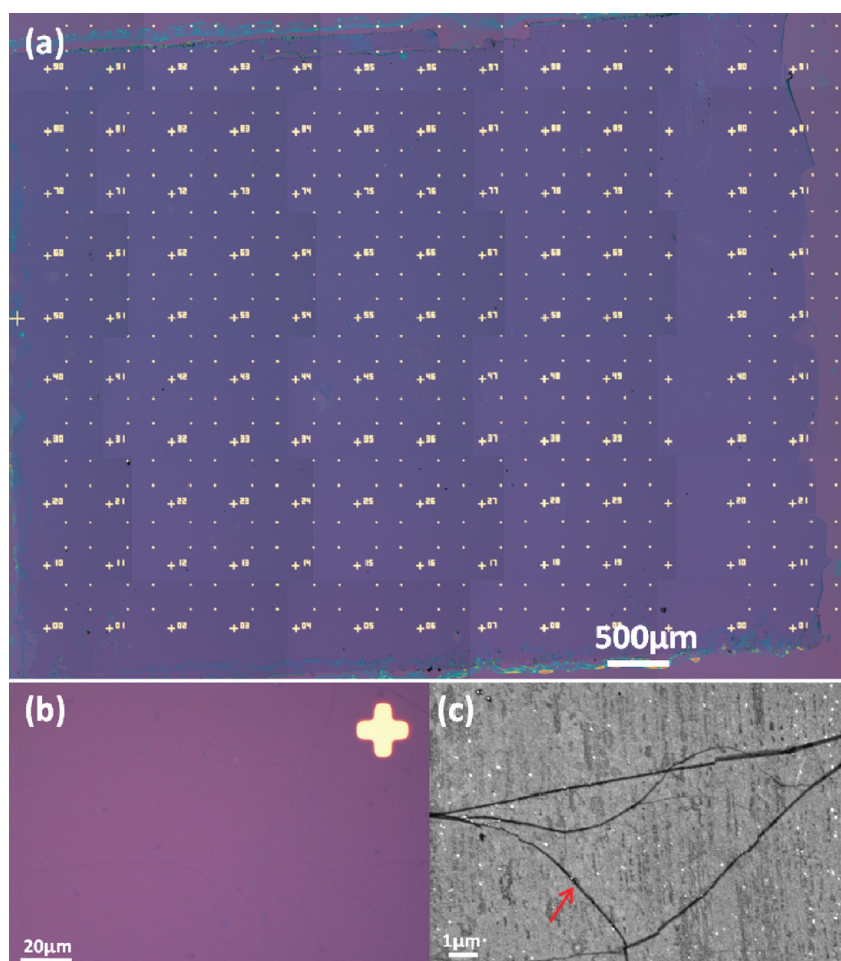


Figure 2. (a) Optical image of a graphene film on Si/SiO₂ substrate transferred with “RCA clean” steps. The tear in the middle of the upper side was introduced by tweezers when handling the sample before Cu etching. (b) Typical high-magnification optical and (c) SEM images of the films shown in (a). The large metal residues shown in Figure 1 are rarely observed. The narrow, dark lines (red arrow) are wrinkles.

the micrographs. These lines are attributed to wrinkles formed during the growth process.⁵ When graphene is transferred onto a substrate, these wrinkles collapse and narrow multilayer graphene stripes form, which show higher contrast in both optical and SEM images. This formation is similar to the formation of larger folds, which will be discussed later in this paper.

To further confirm the cleanliness of the RCA clean process, X-ray photoelectron spectroscopy (XPS) was used to characterize the contamination and the transferred graphene films. Figure 3 shows the Cu 2p high-resolution XPS spectra obtained from two transferred samples (A and B) and a sample mechanically exfoliated from natural graphite (C) as a Cu-free control. The RCA clean of sample A was carried out at room temperature for 15 min of each SC step, while sample B was cleaned at 0 °C for 30 min of each step to further reduce the reaction aggressiveness and protect the PMMA/graphene stacks from tearing. The spectra of sample A are very similar to the spectra obtained from the exfoliated sample C. No Cu is observed on these films to the resolution limit of the instrument, indicating

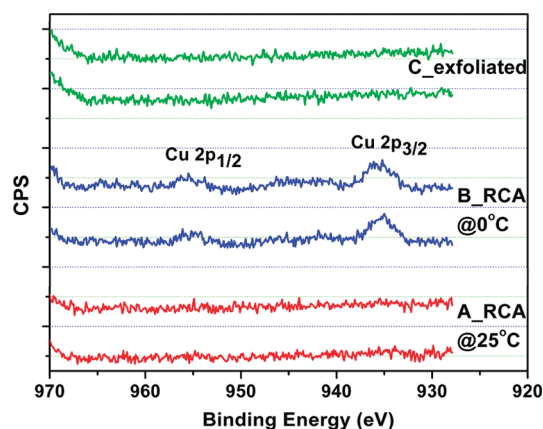


Figure 3. High-resolution XPS spectra of the Cu 2p region obtained from two transferred samples (A and B) and a sample (C) mechanically exfoliated from natural graphite as a control. Spectra were recorded at two different positions on each sample.

that a 15 min per step RCA clean at room temperature effectively removes all of the Cu contamination remaining after Cu substrate etching. Sample B spectra show small Cu peaks, indicating that a small quantity of

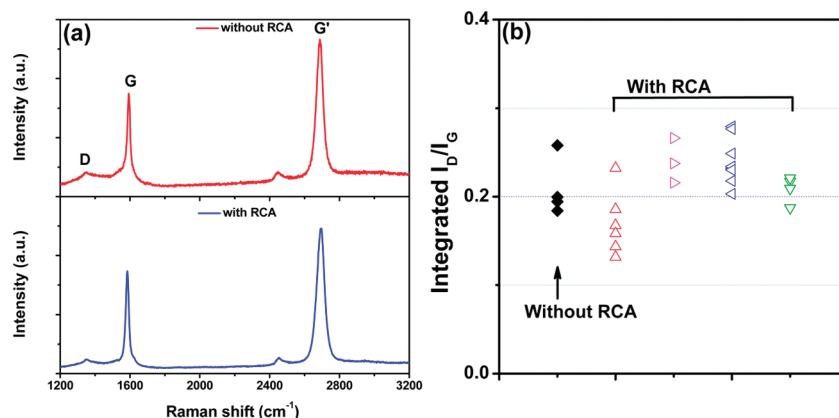


Figure 4. (a) Typical Raman spectra of graphene transferred with and without RCA clean steps after Cu etching. (b) Comparison results of the integrated Raman intensity ratio, I_D/I_G , between a sample transferred without an RCA clean and four samples transferred with the RCA clean. All graphene samples were grown from the same Cu substrate, and all data were measured on monolayer graphene regions.

Cu contamination remains. These results support the claim that the large residual particles, which were difficult to completely remove in the Cu-etch solutions as shown in Figure 1, are likely Cu residues. These Cu residues are effectively cleaned by the RCA process; however, the etching temperature and solution concentration must be well controlled. For example, lower concentrations and lower temperatures slow the chemical reactions and “cleaning rates”, which help preserve the PMMA/graphene stack from mechanical damage or tearing, but it takes a longer time to thoroughly clean the Cu contamination on the graphene film. Our results indicate 15 min per step RCA etching at room temperature with 20:1:1 RCA solutions is a good choice to effectively clean transferred graphene. There is no indication of Fe on the films in the XPS spectra, which strongly suggests that Fe contamination from the etching solution is effectively cleaned by a thorough DI rinse and/or RCA clean protocols.

The primary concern of the “RCA clean” transfer process is whether the graphene is degraded by the RCA cleaning steps. Raman spectroscopy is a powerful tool to characterize the structure and defects of carbon materials including carbon nanotubes and graphene.¹⁴ Figure 4a shows typical Raman spectra of graphene that had been transferred with and without RCA clean steps after Cu etching. Disorder in a graphene monolayer can be quantified by analyzing the intensity ratio between the disorder-induced D band and the Raman-allowed G band (I_D/I_G).¹⁴ A higher I_D/I_G value indicates more defects in graphene. Figure 4b shows a comparison of the I_D/I_G ratio between a sample prepared without an RCA cleaning step and four samples prepared with the RCA clean. All of these graphene samples were cut from the same Cu growth substrate. They were all grown in the same growth run; thus it is reasonable to assume they have a similar initial defect density. The polycrystalline nature of the Cu substrate may affect the graphene growth and induce structural

inhomogeneities in the resulting graphene film. Raman spectra were therefore measured randomly on several positions in the clean monolayer area on each sample. The local inhomogeneities of the graphene lead to a range of I_D/I_G values for each sample (Figure 4b). Compared with the sample transferred without RCA cleaning steps, the ones that underwent a RCA clean process have a similar or lower I_D/I_G ratio. Therefore, the RCA clean process does not noticeably increase the density of defects in the transferred graphene, and the quality of the graphene was not degraded significantly. Raman measurements were also used to characterize doping in graphene.^{15,16} However, due to the drying and baking processes in the clean process and limited measurements on the sample without RCA cleaning steps, no definite conclusion can be drawn on the effect of the RCA clean on the doping level of transferred graphene (see Supporting Information S4).

As mentioned before, a good transfer process produces graphene that will not only be clean without contamination (see Supporting Information S5) but also be continuous without cracks or tears. To obtain a crackless transferred graphene film, the as-grown graphene film on Cu must first be continuous without cracks (see Supporting Information Figure S6). No cracks or folds should be induced in this good starting material during the chemical etching, cleaning, and transfer process. Experimentally, to transfer graphene, the PMMA/graphene stack was scooped out of DI water by the target substrate after Cu etching and RCA clean steps and then allowed to dry. It has been reported that graphene films tend to break at the last PMMA removal step.¹¹ When transferred from water to the target substrate, the PMMA/graphene stack does not make full contact with the SiO_2/Si substrate, and the unattached regions tend to break and form cracks that remain when the PMMA film is dissolved away.¹¹ Usually two kinds of gaps are found between the PMMA/graphene stack and the target substrate due

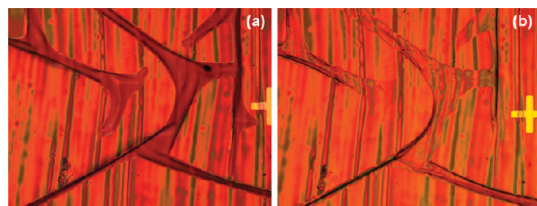


Figure 5. Optical images of large folds before (a) and after (b) baking at 150 °C.

to their incomplete contact. As reported,¹¹ one type of gap arises because the surface of the metal goes through significant surface reconstruction at high temperatures, giving rise to a metal surface that tends to be rough. The graphene follows the surface of the underlying metal. When the Cu is etched away, the PMMA/graphene stack replicates the surface morphology of the Cu and does not lie flat on top of the target surface. Thus, there are always some “small” gaps between the graphene and the substrate surface. Another type of gap forms when water trapped between the stack and the substrate dries. In this case, much “larger” gaps between the PMMA/graphene stack and the substrate form, causing large folds and/or wrinkles, as shown in Figure 5a (see also Supporting Information Figure S7a and Supporting video 1). A second PMMA coating step has been introduced to relax the underlying graphene by partially or fully dissolving the precoated PMMA and leading to better contact with substrate.¹¹ We found this approach is relatively effective for reducing the first category of gap (*i.e.*, the “small” gaps); however, many of the second type of gaps, which are much “larger”, remain. These wrinkles tend to crack during PMMA removal (see Supporting Information Figure S7d). Thus, while the second PMMA coating step reduces the amount of cracking in transferred graphene, it does not completely remove these detrimental defects.

When water between the graphene and the substrate dries, the water surface tension will drag the film into contact with the substrate. Due to the roughness of the stack, a small amount of water may remain in the gaps (both “small” and “large” gaps) between the graphene and the substrate. To dry the residual water thoroughly, the sample was baked at 150 °C for 15 min to evaporate it and improve the contact between the stack and the substrate. Figure 5a and b show images of dried PMMA/graphene stacks before and after this 150 °C baking step. The surface roughness of the transferred PMMA/graphene stack is greatly reduced after baking, indicating the improved contact between the graphene and the substrate. This improvement is most notable for the large-area gaps. As an indication of the improved graphene/substrate contact, we found that the PMMA/graphene stack remains adhered to the target substrate when it is dipped in DI water. After air drying alone, the stack can be released during a DI water dip. It was found that the number of cracks

observed after the PMMA was removed by acetone is greatly reduced by this 150 °C baking step as compared to samples prepared without this baking step (see Supporting Information Figure S7b,c). We found that the 150 °C baking step is more effective at reducing the number of cracks than applying a second PMMA layer. Once the sample is baked, the second PMMA step is not necessary. Typically after PMMA removal, a second bake at 200 °C¹⁷ for 10 min is used to further improve the graphene/substrate contact. These two baking steps were found to be important in determining the end yield of electrical devices fabricated from the graphene films, as will be discussed later.

We have shown that wrinkles or folds will form in transferred graphene/PMMA stacks during water drying. These folds tend to break, creating cracks in the graphene. Although baking (and, to a lesser effect, a second PMMA layer) reduces the folding and cracking in transferred graphene, it cannot totally remove these detrimental defects. This folding can lead to areas of multiply folded graphene, referred to as grafold, which can manifest electronic properties that are different from those of monolayer graphene.¹⁸ While there may be instances when the unique properties of grafold could be harnessed for special applications, in most cases, a flat transfer without folds or cracks is desired. Because the folds form during the water-drying process, it is expected that the hydrophilicity of the surface of the substrate onto which the graphene/PMMA stack will be transferred will have a crucial impact on the formation of the folds. A hydrophilic surface will spread the water more evenly during transfer and improve the smoothness of the graphene/PMMA stack. The surface of a thermally grown SiO₂ surface in normal ambient is hydrophilic. A brief HF dip (50:1 DI/HF) will further increase its hydrophilicity due to an increase in the density of the OH groups on the SiO₂ surface (see Supporting Information Figure S8a).^{19,20} The increase in the hydrophilicity significantly reduces the formation of large folds and wrinkles, and the PMMA/graphene stack can be transferred without large fold formation at all (see Supporting Information Figure S8b). Therefore, cracks arising at those folding areas are avoided completely. We have demonstrated that such a full contact between a PMMA stack and a Si/SiO₂ substrate can be obtained on a silicon wafer with a diameter of up to 150 mm (see Supporting Information Figure S8c). These results imply that crackless transfer of graphene, up to 6 in., is possible, and it is likely that it is possible to transfer much larger areas if larger substrate materials are available. Other techniques that can increase the hydrophilicity of the targeting substrate will have similar effects on reducing the folds and cracks. For example, oxygen plasma treatments also increase the hydrophilicity of SiO₂ substrates.^{19,20} The hydrophilicity of the substrate affects the performance

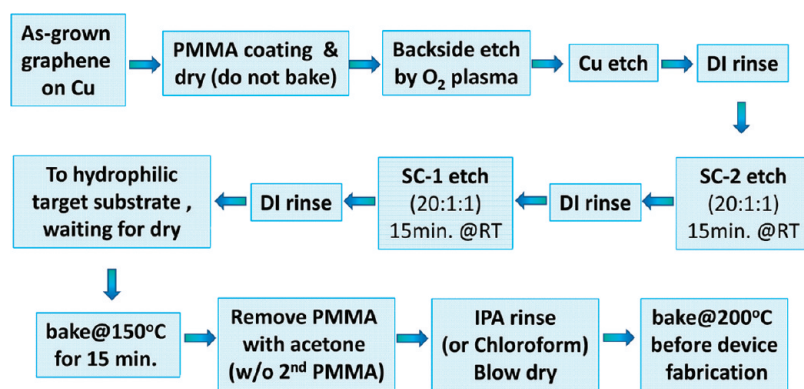


Figure 6. “Modified RCA clean” graphene transfer process flow used here.

of the graphene devices on it through the interaction between the substrate and graphene film.^{19–21} It is reported that the plasma treatment will greatly increase the number of charged defects in the SiO₂ and have a negative effect on the mobility of fabricated devices, while high performance devices can be obtained on HF dip-treated substrates.^{19,20} Thus, the HF dip is our preferred approach for oxidized Si substrates.

On the basis of the results of these extensive experiments probing the effects of cleaning, drying, and surface hydrophilicity, we propose the “modified RCA clean” graphene transfer process flow as shown in Figure 6. Following this process, a clean and almost crackless graphene film can be transferred to various target substrates.

After graphene has been successfully transferred onto Si/SiO₂ substrates, it is ready to be fabricated into electronic devices. In this work, field effect transistors (FETs) were fabricated by standard photolithography from clean, crackless graphene films transferred *via* the modified RCA clean process flow. The graphene film was first patterned into $(6 \times 20) \mu\text{m}^2$ stripes by using an oxygen plasma. Metal source/drain contacts were patterned to form FETs with a $(6 \times 10) \mu\text{m}^2$ channel area where the Si-substrate was used as a back gate. Figure 7 shows images and corresponding electrical measurement results for a typical FET. Figure 7b shows the drain current, I_d , as a function of the drain voltage, V_d , measured at a gate voltage of 0 V for various V_d sweeping ranges. These curves were measured following metal contact lift-off without any postfabrication treatment, such as thermal or current annealing. All curves overlap, indicating that the contact between the source/drain metal and graphene is very stable. Figure 7c and d are field effect measurement results. The transfer characteristic curve (I_d as a function of back gate voltage, V_g) is smooth with little hysteresis, and the conductivity minimum associated with the Dirac point is near 0 V. These results indicate that the surface contamination due to the graphene transfer process is very low; therefore, the device performance is repeatable without any annealing treatment (thermal or current) needed.

To study the uniformity of devices fabricated from graphene films transferred *via* the modified RCA clean process, 205 devices were measured and the distribution of the Dirac point and extracted intrinsic carrier density²² of those devices are shown in Figure 8a and c. The Dirac points of most devices range from 4 to 12 V, and most of the intrinsic carrier densities are less than $1 \times 10^{12} \text{ cm}^{-2}$. As a comparison, Figure 8b and d show results of 121 devices fabricated from graphene transferred by using the traditional process (Fe(NO₃)₃ etch and a second PMMA application without an RCA clean and baking). Most values of Dirac points and intrinsic carrier densities are much higher than those in Figure 8a and c, and their distribution ranges are much wider. This demonstrated that the device uniformity was improved by the modified RCA clean process flow. Furthermore, the lower intrinsic carrier densities shown in Figure 8c indicate the doping of the graphene was reduced by the RCA cleaning steps, although it is not obvious from the Raman measurements. The extracted room-temperature mobilities of most devices fabricated *via* the modified RCA clean method are concentrated between 1000 and 1400 cm²/(V s). Although the mobility is still lower than the best reported mobility of CVD grown graphene,⁹ it is about 2–3 times higher than the devices fabricated *via* the traditional transfer method (which are concentrated around 200–800 cm²/(V s)). This indicates that when the residue particles were removed, the local scattering to the carrier was reduced and hence the mobility was improved. Considering our graphene growth process is nonoptimized and there are defects in the as-grown graphene films, the mobility obtained by the modified RCA clean method can be enhanced much further when the growth process was optimized and the quality of as-grown graphene was improved.

Device yield, which was usually defined by devices with no current, is very important to large-scale device fabrication. After device fabrication, hundreds of devices were measured randomly, and the device yield results were shown in Figure 9. Figure 9a shows the total yield of devices fabricated *via* the modified RCA

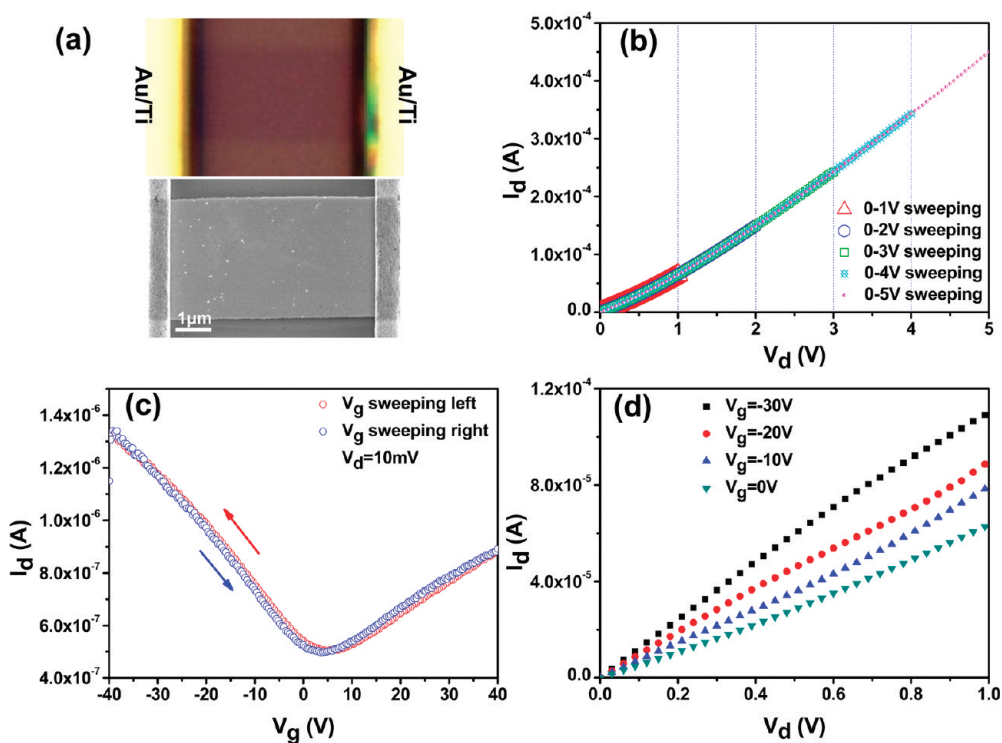


Figure 7. Electrical properties of a FET fabricated from graphene transferred by using the “modified RCA clean” method. (a) Optical and SEM images of a typical FET. (b) I_d – V_d curves measured at $V_g = 0$ V with various V_d sweeping ranges. Typical transfer (c) and output (d) properties of graphene FETs.

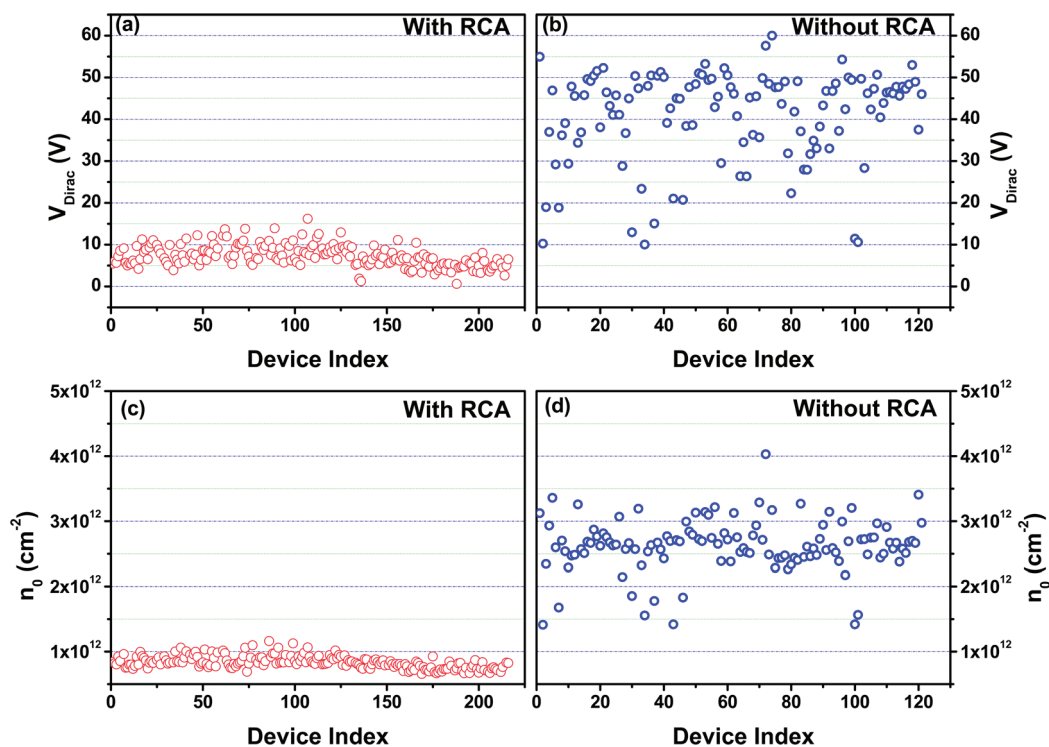


Figure 8. Distribution of Dirac points (a, b) and intrinsic carrier densities (c, d) of devices fabricated from graphene transferred with (a, c) and without (b, d) RCA cleaning steps.

clean flow was over 97%, and those of the traditional transfer method is about 94%, which is slightly lower, as shown in Figure 9b. Our characterization indicates

that the device yield was determined primarily by cracks in the graphene film. To be specific, larger and multiple cracks that completely cross the width of the

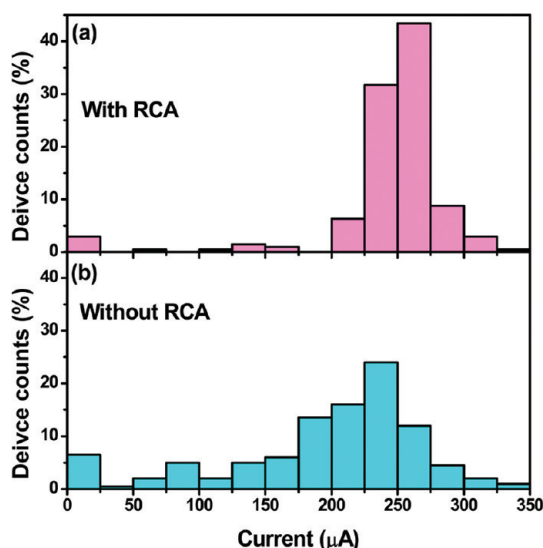


Figure 9. Device yields and output current distribution of devices fabricated from graphene transferred by (a) the “modified RCA clean” method and (b) the traditional “PMMA-mediated” method. The output currents were recorded at $V_d = 3$ V and $V_g = 0$ V.

device channel lead to open circuit devices and subsequently to lower device yields (see Supporting Information S9). The HF dip treatment, which increases the hydrophilicity of the substrate and reduces large cracks, therefore directly increases device yield. In addition to the “large” cracks, small sub-micrometer cracks and holes may form during the transfer, which cannot be seen in optical images but are revealed by SEM images (see Supporting Information S9). Therefore a device that appears “good” under an optical microscope may have small cracks and holes within the channel. These cracks and holes diminish the output current through the device and increase the spread in the current distribution. The output current distribution of devices in Figure 9a is much narrower than that in Figure 9b. This indicates the number of devices that have cracks and holes in their channel was greatly reduced. SEM observation confirmed this conclusion (see Supporting Information S9a,b). It is also found that almost no cracks or holes were observed in the channel of devices with an output current greater than $200 \mu\text{A}$ for the $(6 \times 10) \mu\text{m}^2$ channel; therefore such devices were regarded as “good devices”. The good device in Figure 9a is about 93.6%, while only 59.5% in Figure 9b.

METHODS

Graphene was grown on $25 \mu\text{m}$ thick Cu foils by using CVD methods.⁵ After growth, a PMMA solution (molecular weight 495 000 g/mol, 4% by volume dissolved in anisole) was spin coated onto the top side of the sample at 1000 rpm. Then the PMMA film, with thickness about 300 nm, was kept at room temperature for 12 h to dry. Typically, graphene will grow on both sides of a Cu foil and the back-side graphene will hinder

This demonstrates these smaller defects, which are so detrimental to output current, can be greatly reduced by using the simple baking steps described earlier. Device yields over 90% previously have been reported,^{23–25} however, device yield alone cannot fully characterize the quality of a graphene transfer process. Both device yield and electrical uniformity are important parameters for evaluating the effectiveness of a graphene transfer method. The reduction of Cu residues on graphene by using the RCA clean steps results in a clean graphene surface, which impacts the electrical contact stability and contributes to the narrow distributions shown in Figure 8a,c. The use of HF to control the hydrophilicity of the target sample surface to minimize large cracks and adding baking steps to improve the graphene/substrate contact contribute to improving the yield of good devices and uniformity shown in Figure 9.

CONCLUSIONS

In summary, we have systematically studied wet-chemical methods for transferring graphene from Cu substrates to target substrates. On the basis of the results of this study, we have developed a “modified RCA clean” process for the transfer of CVD graphene. Cu and/or Fe contamination, which is difficult to remove completely by conventional transfer methods, is thoroughly cleaned by the modified RCA clean steps. The graphene/target-substrate interface resulting from this clean transfer process is greatly improved. Since the RCA clean is effective for many kinds of metal contaminations, our proposed transfer process can be generalized to transfer graphene grown on other metals besides Cu and Ni. In addition, we demonstrated that the number of cracks in transferred graphene films can be reduced by controlling the hydrophilicity of the target substrate and baking. By combining an effective metal cleaning process (the modified RCA clean) with control of the hydrophilicity of the target substrates, we have developed and demonstrated a transfer process that can improve both device yield and performance uniformity. Though the transfer process was demonstrated on silicon substrates in this paper, it can be generalized to other types of substrates. This process paves the way toward the clean and crackless transfer of graphene and could enable large-scale device production.

the Cu etch process. The back-side graphene was removed by oxygen plasma etching for 3 min at a power of 100 W. The Cu substrate under the graphene film was etched in an iron nitrate solution with a concentration of about 0.7 mol/L in water.

The silicon substrates used in this work were highly p-doped with about 285 nm oxide. Raman spectra were acquired under ambient conditions with a Renishaw InVia micro-Raman spectrometer²⁶ equipped with a 514 nm (2.41 eV) wavelength excitation laser and an

1800 lines/mm grating while operating in 180° backscattering geometry. A 50× objective was used to focus the excitation laser light spot of approximately 2 μm on the graphene samples with an on-sample incident power of less than 2 mW to avoid local heating effects. X-ray photoemission spectra were taken at a Kratos Axis Ultra DLD equipped with a monochromatized Al X-ray source providing Al Kα radiation with a line width of 0.3 meV.

Graphene FETs were fabricated by standard photolithography processes based on a widely used photoresist, Shipley 1813. A descum process was not used prior to metal deposition. The oxygen plasma in the descum process will damage the one-atom-thick graphene film. After metal deposition, lift-off was performed at 80 °C by soaking the sample in Microposit Remover 1165 (1-methyl-2-pyrrolidinone) and then thoroughly rinsed with isopropyl alcohol. This process will strip the photoresist from the graphene surface relatively cleanly. No post-processing annealing was performed.²⁷ Electrical properties of the final devices were measured under vacuum by using an Agilent 4156C semiconductor parameter analyzer.

Acknowledgment. We acknowledge Dr. Houxun Miao and Dr. Lei Chen for their experimental help and Dr. Tian Shen for assistance with data analysis. X.L. was partially supported by the Ministry of Science and Technology of China (Grant No. 2011CB921904) and National Natural Science Foundation of China (Grant No. 60971003). Q.L. would like to acknowledge the support of George Mason University Seed Fund. The authors thank the NIST Center for Nanoscale Science and Technology's Nanofab Facility for device fabrication support, and Dr. Luigi Colombo of Texas Instruments for helpful discussions and suggestions.

Supporting Information Available: More detailed optical and SEM images of graphene transferred by traditional and the “modified RCA clean” method; images of as-grown graphene samples; Raman data analysis of graphene transferred with and without RCA clean; cleaning the top surface of graphene; growth discontinuity and the formation of nanoscrolls; 150 °C baking treatment; effect of substrate hydrophilicity; device morphology and the effect of baking at 200 °C. This material is available free of charge via the Internet at <http://pubs.acs.org>.

REFERENCES AND NOTES

- ITRS, International Technology Roadmap for Semiconductors, 2009. <http://www.itrs.net>.
- Avouris, Ph. Graphene: Electronic and Photonic Properties and Devices. *Nano Lett.* **2010**, *10*, 4285–4294.
- Novoselov, K. S.; Geim, A. K.; Morozov, S. V.; Jiang, D.; Zhang, Y.; Dubonos, S. V.; Grigorieva, I. V.; Firsov, A. A. Electrical Field Effect in Atomically Thin Carbon Films. *Science* **2004**, *306*, 666–669.
- Berger, C.; Song, Z. M.; Li, T. B.; Li, X. B.; Ogbazghi, A. Y.; Feng, R.; Dai, Z. T.; Marchenkov, A. N.; Conrad, E. H.; First, P. N.; de Heer, W. A. Ultrathin Epitaxial Graphite: 2D Electron Gas Properties and a Route toward Graphene-Based Nanoelectronics. *J. Phys. Chem. B* **2004**, *108*, 19912–19916.
- Li, X.; Cai, W.; An, J.; Kim, S.; Nah, J.; Yang, D.; Piner, R.; Velamakanni, A.; Jung, I.; Tutuc, E.; Banerjee, S.; Colombo, L.; Ruoff, R. S. Large-Area Synthesis of High-Quality and Uniform Graphene Films on Copper Foils. *Science* **2009**, *324*, 1312–1314.
- Kim, K. S.; Zhao, Y.; Jang, H.; Lee, S. Y.; Kim, J. M.; Kim, K. S.; Ahn, J.; Kim, P.; Choi, J.; Hong, B. H. Large-Scale Pattern Growth of Graphene Films for Stretchable Transparent Electrodes. *Nature* **2009**, *457*, 706–710.
- Taghioskoui, M. Trends in Graphene Research. *Mater. Today* **2009**, *12*, 34–37.
- Bae, S.; Kim, H.; Lee, Y.; Xu, X.; Park, J.; Zheng, Y.; Balakrishnan, J.; Lei, T.; Kim, H. R.; Song, Y. I.; *et al.* Roll-to-Roll Production of 30-in. Graphene Films for Transparent Electrodes. *Nat. Nanotechnol.* **2010**, *5*, 574–578.
- Li, X.; Magnuson, C. E.; Venugopal, A.; An, J.; Suk, J. W.; Han, B.; Borysiak, M.; Cai, W.; Velamakanni, A.; Zhu, Y.; *et al.* Graphene Films with Large Domain Size by a Two-Step Chemical Vapor Deposition Process. *Nano Lett.* **2010**, *10*, 4328–4334.
- Reina, A.; Son, H.; Jiao, L.; Fan, B.; Dresselhaus, M. S.; Liu, Z. F.; Kong, J. Transferring and Identification of Single- and Few-Layer Graphene on Arbitrary Substrates. *J. Phys. Chem. C* **2008**, *112*, 17741.
- Li, X.; Zhu, Y.; Cai, W.; Borysiak, M.; Han, B.; Chen, D.; Piner, R.; Colombo, L.; Ruoff, R. S. Transfer of Large-Area Graphene Films for High-Performance Transparent Conductive Electrodes. *Nano Lett.* **2009**, *9*, 4359.
- Jiao, L.; Fan, B.; Xian, X.; Wu, Z.; Liu, Z. F. Creation of Nanostructures with Poly(methyl methacrylate)-Mediated Nanotransfer Printing. *J. Am. Chem. Soc.* **2008**, *130*, 12612–12613.
- Handbook of Semiconductor Cleaning Technology*; Kern, W., Ed.; Noyes Publishing: Park Ridge, NJ, 1993; Chapter 1.
- Dresselhaus, M. S.; Jorio, A.; Hofmann, M.; Dresselhaus, G.; Saito, R. Perspectives on Carbon Nanotubes and Graphene Raman Spectroscopy. *Nano Lett.* **2010**, *10*, 751–758.
- Das, A.; Pisana, S.; Chakraborty, B.; Piscanec, S.; Saha, S. K.; Waghmare, U. V.; Novoselov, K. S.; Krishnamurthy, H. R.; Geim, A. K.; Ferrari, A. C.; Sood, A. K. Monitoring Dopants by Raman Scattering in an Electrochemically Top-Gated Graphene Transistor. *Nat. Nanotechnol.* **2008**, *3*, 210–215.
- Kalbac, M.; Reina-Cecco, A.; Farhat, H.; Kong, J.; Kavan, L.; Dresselhaus, M. S. The Influence of Strong Electron and Hole Doping on the Raman Intensity of Chemical Vapor-Deposition Graphene. *ACS Nano* **2010**, *4*, 6055–6063.
- Cheng, Z.; Zhou, Q.; Wang, C.; Li, Q.; Wang, C.; Fang, Y. Toward Intrinsic Graphene Surfaces: A Systematic Study on Thermal Annealing and Wet-Chemical Treatment of SiO₂-Supported Graphene Devices. *Nano Lett.* **2011**, *11*, 767–771.
- Kim, K.; Lee, Z.; Malone, B.; Chan, K. T.; Regan, W.; Gannett, W.; Alemán, B.; Crommie, M. F.; Cohen, M. L.; Zettl, A. Multiply Folded Graphene. *arXiv:1012.5426*
- Nagashio, K.; Yamashita, T.; Fujita, J.; Nishimura, T.; Kita, K.; Toriumi, A. Impacts of Graphene/SiO₂ Interaction on FET Mobility and Raman Spectra in Mechanically Exfoliated Graphene Films. *IEEE Elect. Dev. Meeting (IEDM)* **2010**, 23.4.1–23.4.4.
- Nagashio, K.; Yamashita, T.; Nishimura, T.; Kita, K.; Toriumi, A. Electrical Transport Properties of Graphene on SiO₂ with Specific Surface Structures. *J. Appl. Phys.* **2011**, *110*, 024513.
- Lafkoti, M.; Krauss, B.; Lohmann, T.; Zschieschang, U.; Klauk, H.; Klitzing, K.; Smet, J. Graphene on a Hydrophobic Substrate: Doping Reduction and Hysteresis Suppression under Ambient Conditions. *Nano Lett.* **2010**, *10*, 1149–1153.
- Kim, S.; Nah, J.; Jo, I.; Shahrijerdi, D.; Colombo, L.; Yao, Z.; Tutuc, E.; Banerjee, S. Realization of a High Mobility Dual-Gated Graphene Field-Effect Transistor with Al₂O₃ Dielectric. *Appl. Phys. Lett.* **2009**, *94*, 062107.
- Levendorf, M. P.; Ruiz-Vargas, C. R.; Grag, S.; Park, J. Transfer-Free Batch Fabrication of Single Layer Graphene Transistors. *Nano Lett.* **2009**, *9*, 4479–4483.
- Lee, Y.; Bae, S.; Jang, H.; Jang, S.; Zhu, S.; Sim, S. K.; Song, Y. I.; Hong, B. H.; Ahn, J. H. Wafer-Scale Synthesis and Transfer of Graphene Films. *Nano Lett.* **2010**, *10*, 490–493.
- van der Zande, A. M.; Barton, R. A.; Alden, J. S.; Ruiz-Vargas, C. S.; Whitney, W. S.; Pham, P.; Park, J.; Parpia, J. M.; Craighead, H. G.; McEuen, P. L. Large-Scale Arrays of Single-Layer Graphene Resonators. *Nano Lett.* **2010**, *10*, 4869–4873.
- Certain commercial equipment, instruments, or materials are identified in this paper in order to specify the experimental procedure adequately. Such identification is not intended to imply recommendation or endorsement by the National Institute of Standards and Technology, nor is it intended to imply that the materials or equipment identified are necessarily the best available for the purpose.
- It is known that postprocessing annealing can remove resist residue on the graphene channel and improve the device performance. We do not apply such postprocessing annealing here. Our concern is that the annealing process is usually performed in a hydrogen environment and hydrogen may react with the metal contact and change its work function. Therefore the contact between the metal and graphene is likely to be modified, which may complicate the analysis of the results.